


Research Article

# Study of Metoprolol-Loaded Poly(Lactic-co-Glycolic Acid)–Poly(Trimethylene Carbonate)–Poly(Glycolic Acid) Drug-Eluting Stents for Coronary Heart Disease

Rongrong Lu<sup>1,\*</sup>, Aimaitijiang Maimaiti<sup>1</sup>, Tuohetiajimu Abudurehman<sup>1</sup>

<sup>1</sup>Department of Cardiology CCU, Kashi Prefecture Second People's Hospital, 844000 Kashi, Xinjiang, China

\*Correspondence: [lurongksshgar@163.com](mailto:lurongksshgar@163.com) (Rongrong Lu)

Academic Editor: Mehmet Ozaslan

Published: 22 September 2025

## Abstract

**Background and Objective:** Drug-eluting stents (DES) have become a crucial strategy for improving the outcomes of patients with coronary artery disease (CAD). This work aimed to evaluate the therapeutic efficacy of metoprolol-loaded poly (lactic-co-glycolic acid)–poly(trimethylene carbonate)–poly (glycolic acid) (PLGA–PTMC–PGA) DES (Meto-PLGA/PTMC DES) in a rabbit model of CAD. **Methods:** A total of 30 New Zealand white rabbits (male, weighing 4–6 kg) were randomly divided into three groups: Sham group (chest suturing without intervention), Model group (CAD animal model without DES), and stent group (treatment with the Meto-PLGA/PTMC DES). The blood samples were collected at regular intervals to assess the serum inflammatory markers, cardiac function parameters, hemodynamic parameters and coronary remodeling. Statistical analysis was performed using One-way analysis of variance (ANOVA), followed by a *post hoc* Tukey's test to compare the differences between groups ( $p < 0.05$  indicated statistical significance). **Results:** The Meto-PLGA/PTMC DES, through its unique co-polymer structure, achieved stable Meto loading *in vivo*. This stent enabled the gradual release of Meto, thus maintaining sustained drug concentrations and optimizing CAD treatment. The animal experiment results indicated that the stent group (Meto-loaded DES) exhibited markedly lower levels of interleukin-8 (IL-8), tumor necrosis factor- $\alpha$  (TNF- $\alpha$ ), vascular cell adhesion molecule-1 (VCAM-1), and intercellular adhesion molecule-1 (ICAM-1) relative to the model group ( $p < 0.05$ ). In terms of cardiac function, compared with the model group, the stent group exhibited significantly elevated left ventricular systolic pressure (LVSP),  $\pm dp/dt_{max}$ , arterial systolic blood pressure (BPs), and diastolic blood pressure (BPd), along with a marked reduction in left ventricular end-diastolic pressure (LVEDP) compared with the model group ( $p < 0.05$ ). The coronary tissue morphology in the stent group revealed notably reduced intimal thickness, intimal area and degree of stenosis versus the Model group, with a prominent increase in lumen area ( $p < 0.05$ ). **Conclusion:** The Meto-PLGA/PTMC DES not only effectively provides sustained drug release and exhibits superior mechanical properties and excellent blood compatibility. Animal experiments further validated the crucial role of the Meto-PLGA/PTMC DES in reducing inflammatory responses, improving cardiac function and alleviating coronary artery stenosis.

**Keywords:** Metoprolol; drug-eluting stent; cardiovascular diseases; sustained-release medication; inflammation

## 1. Introduction

Coronary artery disease (CAD) is a leading cause of mortality and disease burden [1]. The CAD results in myocardial ischemia and cardiac functional impairment, posing a considerable threat to life and health [2]. Although percutaneous coronary intervention with stenting is widely adopted due to its minimal invasiveness and rapid recovery, conventional bare-metal stents are prone to restenosis and thrombotic complications [3,4]. Consequently, drug-eluting stents (DES) have increasingly become a focal point of research in recent years [5–7].

The DES have been applied for treating cardiovascular diseases, particularly demonstrating marked efficacy in preventing coronary artery restenosis [8]. Conventional DES typically loads antiproliferative drugs, such as sirolimus or paclitaxel, to inhibit neointimal hyperplasia [9]. However, the potential of  $\beta$ -blockers like Metoprolol (Meto)

to reduce cardiovascular event rates has garnered research interest. Meto, a widely utilized  $\beta$ -blocker, effectively reduces cardiovascular events by lowering heart rate and blood pressure (BP) while also exerting anti-inflammatory effects, making it a promising candidate for improving patient outcomes when incorporated into DES [10,11]. Traditional oral administration methods face challenges such as rapid drug metabolism, short duration of effect and poor patient compliance, which limit their application in chronic cardiovascular disease treatment. Against this backdrop, researchers have begun exploring the integration of Meto with stents to achieve localized sustained release via DES, aiming to extend drug action time, reduce cardiovascular event rates and lower the risk of coronary artery restenosis [12]. Research on Meto-eluting stents is still in its early stages. Existing studies primarily focused on optimizing stent materials and drug release systems to achieve stable and sustained release of Meto with prolonged ef-



ficacy. Poly (lactic-co-glycolic acid)-poly (trimethylene carbonate)-poly (glycolic acid) (PLGA-PTMC-PGA) is an emerging biodegradable material that, due to its excellent mechanical properties, biocompatibility and controllable degradation, represents an ideal matrix for DES [13]. By loading Meto onto a PLGA-PTMC-PGA DES (Meto-PLGA/PTMC DES), researchers aimed to achieve localized sustained drug release, reducing systemic side effects and extending the duration of action. The Meto-PLGA/PTMC DES facilitates the controlled release of Meto, thereby maintaining its cardiovascular event-reducing effects and effectively decreasing the risks of thrombosis and restenosis following stent implantation. Additionally, the biodegradable nature of this stent obviates the need for permanent implants, thereby minimizing long-term risks associated with permanent devices and eliminating the need for secondary surgical removal, thus reducing procedural risks and costs. Combined with Meto's anti-inflammatory and anti-myocardial remodeling effects, this DES holds promise for improving overall outcomes in patients with CAD, particularly those at high risk. Thus, Meto-PLGA/PTMC DES represents not only a novel therapeutic strategy but also a significant advancement in stent technology.

To address these issues, this work developed a Meto-PLGA/PTMC DES using PLGA-PTMC-PGA as the material. This novel DES controls the slow release of the drug, maintaining stable drug concentrations over extended periods and thereby enhancing therapeutic efficacy. Additionally, the Meto-PLGA/PTMC DES exhibited excellent biocompatibility and degradability, gradually breaking down into non-toxic byproducts that are fully absorbed and metabolized by the body. This work aimed to explore the adoption potential of this DES in the treatment of cardiovascular diseases and to evaluate its impact on the efficacy and safety of Meto.

## 2. Materials and Methods

### 2.1 Study Area

The study was conducted at Kashi Prefecture Second People's Hospital (Xinjiang, China) from May, 2023 to March, 2024.

### 2.2 Synthesis of PLLA-PTMC-PGA Complex

The L-lactic acid (Catalog No. L0165, TCI America, Portland, OR, USA) was employed as the starting material to synthesize lactide oligomers via a dehydration polycondensation methodology. The lactide oligomers were then depolymerized into L-lactide (LLA) under high-temperature vacuum conditions at 50–130 °C. Following crystallization through washing with anhydrous ether and vacuum drying at 35 °C to constant weight, poly LLA (PLLA) was obtained. Using diethyl carbonate (Catalog No. 436131000, Thermo Scientific Chemicals, Waltham, MA, USA) and 1,3-propanediol as raw materials, PTMC oligomers were synthesized through polycondensation un-

der high-temperature vacuum conditions at 180 °C after ethanol removal. The crude product was dissolved in ether and acetone mixture, repeatedly crystallized five times in an ice water bath, washed with anhydrous ether and then vacuum filtered and dried at 25 °C to constant weight, yielding PTMC. Using carboxylic acid as the raw material, the mixture was heated to 140 °C in oil. After dehydration between hydroxy acetic acid molecules, stannous octoate was added under vacuum conditions at 200 °C to yield pale yellow crystals. The product was recrystallized five times using ethyl acetate, washed once with anhydrous ether and vacuum-dried at 35 °C to constant weight, resulting in poly (glycolic acid) (PGA). Under nitrogen protection, PLLA, PTMC, and PGA were melted and mixed uniformly (the mass ratios of PLLA:PTMC:PGA were 1:1:1, 1:1:2 and 1:1:3, respectively), then cooled and solidified in an ice-water bath. The mixture was subjected to vacuum treatment for 3 hrs and reacted at 130 °C for 72 hrs. The copolymer was dissolved in a Dichloromethane solution (Catalog No. D807825, Shanghai Macklin Biochemical Technology Co., Ltd., Shanghai, China), precipitated with ethanol and vacuum-dried at 60 °C to constant weight, yielding the PLLA-PTMC-PGA composite.

### 2.3 Fabrication and Characterization of Meto-PLGA/PTMC DES

A 5% (w/v) solution of PLLA-PTMC-PGA was dissolved in 1,4-dioxane (Catalog No. D116356, Aladdin Industrial Corporation, Shanghai, China) and stirred for 3 hrs using a magnetic stirrer (Catalog No. 85-2, Shanghai Sile Instrument Co., Ltd., Shanghai, China). Deionized water (prepared using a Milli-Q water purification system, Catalog No. Direct-Q 3, Merck KGaA, Darmstadt, Germany) was then applied and stirring continued for an additional 2 hrs. Metoprolol (Meto, Catalog No. M1013, Sigma-Aldrich, St. Louis, MO, USA) was incorporated and stirred for 1 hr to ensure its uniform distribution within the stent material. The temperature was maintained at approximately 5 °C above the cloud point using a constant temperature water bath (Catalog No. HH-S2, Jintan Medical Instrument Factory, Jintan, China) and then slowly decreased to the gel point for 2 hrs. The clear solution was quickly transferred to liquid nitrogen (Nanjing Special Gas Factory Co., Ltd., Nanjing, China) for 1 hr to freeze rapidly, ensuring stable binding of Meto with the material and preventing separation or drug precipitation.

The resulting Meto-PLGA/PTMC DES was obtained through freeze-drying for 24 hrs using a freeze dryer (Catalog No. FD-1A-50, Beijing Boyikang Experimental Instrument Co., Ltd., Beijing, China). The stent material was placed in 10 mL of Dimethyl Sulfoxide (DMSO, Catalog No. D8371, Sigma-Aldrich, St. Louis, MO, USA) and stirred at 37 °C for 1, 3, 6, 12, 24, 48 and 96 hrs using a thermostatic shaker (Catalog No. THZ-320, Shanghai Jinghong Laboratory Equipment Co., Ltd., Shanghai,

China). At each time, 2 mL of release solution was sampled (buffer replenished) and analyzed for Meto release using a UV-1901 ultraviolet Spectrophotometer (Shanghai Lengguang Technology Co., Ltd., Shanghai, China).

#### 2.4 Biocompatibility Testing of Meto-PLGA/PTMC DES

The Meto-PLGA/PTMC DES samples were individually dissolved in dichloromethane (Catalog No. D8418, Sigma-Aldrich, St. Louis, MO, USA) to prepare solutions at 10 ng/mL. As 300  $\mu$ L aliquot of each sample was applied to clean glass slides (Catalog No. 7101, Thermo Fisher Scientific, Waltham, MA, USA), vacuum-dried to constant weight using a vacuum dryer (Catalog No. DZF-6050, Shanghai Jinghong Laboratory Equipment Co., Ltd., Shanghai, China) and then UV-sterilized for 30 min using a UV sterilizer (Catalog No. SW-CJ-2FD, Suzhou Antai Air Technology Co., Ltd., Suzhou, China). The samples were extracted using either physiological saline (Catalog No. P1400, Solarbio Science & Technology Co., Ltd., Beijing, China) or DMEM (Catalog No. 12100046, Thermo Fisher Scientific, Waltham, MA, USA) at a liquid-to-membrane ratio of 1 mL/6 cm<sup>2</sup> for 72 hrs at 37 °C under sterile conditions in a CO<sub>2</sub> incubator (Catalog No. BB15, Thermo Fisher Scientific, Waltham, MA, USA), filtrated through a 0.22  $\mu$ m pore filter (Catalog No. SLGP033RB, Merck Millipore, Darmstadt, Germany). Rabbit cardiac fibroblasts (Catalog No. KL-C1025, Shanghai Kanglang Bio-Tech Co., Ltd., Shanghai, China) were cultured under standard conditions and prepared as a cell suspension at  $1 \times 10^4$  cells/mL. As 100  $\mu$ L aliquot of suspension was seeded in a 96-well plate and incubated for 24 hrs. Cell morphology was observed under an inverted microscope (Catalog No. IX73, Olympus, Japan). The rabbit cardiac fibroblasts exhibited a typical spindle-shaped morphology with uniform size, clear cytoplasm and intact cell membranes, consistent with the characteristic phenotype of fibroblasts. Surface marker identification was performed using flow cytometry (Catalog No. FACSCanto II, BD Biosciences, Sussex, NJ, USA). The cells were positive for vimentin ( $\geq 95\%$ ) and negative for CD31 ( $< 2\%$ ) and  $\alpha$ -smooth muscle actin ( $< 5\%$ ), confirming their identity as cardiac fibroblasts. Mycoplasma detection was conducted using a mycoplasma detection kit (Catalog No. MP0030, Sigma-Aldrich, St. Louis, MO, USA). The result was negative, indicating the absence of mycoplasma contamination in the cell culture. The original medium was then removed and replaced with a 1:1 ratio of medium containing the sample extract. Cells were further incubated for 12, 24, 36, 48 and 96 hrs, with 20  $\mu$ L of a 5 mg/mL methyl thiazolyl tetrazolium (MTT) reagent (Shanghai Enzyme Linked Bio, China) applied. After a 6 hrs incubation, the supernatant was discarded and 150  $\mu$ L of DMSO (Sigma-Aldrich, St. Louis, MO, USA) was applied and shaken for 10 min using a microplate shaker (Catalog No. TS-100, BIOSAN, Riga, Latvia). Absorbance at 570 nm was measured via a mi-

croplate reader (Catalog No. Multiskan FC, Thermo Fisher Scientific, Waltham, MA, USA) and the relative proliferation rate was calculated.

Rabbit blood (Guangzhou Ruite Biotechnology Co. Ltd., China) was anticoagulated and mixed with physiological saline (Catalog No. P1400, Solarbio Science & Technology Co., Ltd., Beijing, China) at a 4:5 ratio. The mixture was centrifuged at 1500 rpm for 10 min using a centrifuge (Catalog No. 5810R, Eppendorf AG, Hamburg, Germany) to collect supernatant. A 10 mL aliquot of the Meto-PLGA/PTMC DES sample extract was incubated at 37 °C for 30 min in a water bath (Catalog No. HH-S4, Jintan Medical Instrument Factory, Jintan, China), mixed with 200  $\mu$ L of fresh anticoagulated blood and incubated for an additional hour. The mixture was centrifuged at 3000 rpm for 5 min using a centrifuge (Catalog No. 5810R, Eppendorf AG, Hamburg, Germany) and the supernatant's absorbance was measured at 540 nm employing a microplate reader (Catalog No. Multiskan FC, Thermo Fisher Scientific, Waltham, MA, USA).

The hemolytic ratio was calculated using [7]:

$$\text{Hemolytic ratio} = \frac{(\text{Sample absorbance} - \text{Saline absorbance})}{(\text{Distilled water absorbance} - \text{Saline absorbance})} \times 100$$

The Meto-PLGA/PTMC DES samples were dissolved in dichloromethane (Catalog No. D8418, Sigma-Aldrich, St. Louis, MO, USA) and evenly coated on the concave center of a glass surface dish (Catalog No. xy085, Shanghai Yubo Biotechnology Co., Ltd., Shanghai, China), then allowed to evaporate at 25 °C. Following this, 200 mL of anticoagulated blood was applied. At 0, 0.25, 0.5, 1 and 2 hrs, the glass surface was gently washed with 100  $\mu$ L of ultrapure water (prepared using a Milli-Q water purification system, Catalog No. Direct-Q 5, Merck KGaA, Darmstadt, Germany) and absorbance at 540 nm was measured via HBS-1101 microplate reader (Nanjing Detie Experimental Equipment Co., Ltd., Nanjing, China).

#### 2.5 Animal Grouping and Treatment

A total of 30 adult male New Zealand white rabbits (4–6 kg) were anesthetized for the procedure using 3% sodium pentobarbital (Catalog No. P3761, Sigma-Aldrich, St. Louis, MO, USA) at a dose of 0.05 g/kg, and the animals were purchased from Shanghai Jiagen Biotechnology Co. Ltd., China. A constriction ring (custom-made, Suzhou Weirui Medical Device Technology Co., Ltd., Suzhou, China) was placed at the distal end of the left coronary artery under assisted breathing conditions using a small animal ventilator (Catalog No. SAR-830, CWE Inc., Ardmore, PA, USA). Post-operative disinfection was performed with 75% ethanol (Catalog No. E7023, Sigma-Aldrich, St. Louis, MO, USA) and anti-inflammatory treatment were administered with ceftriaxone sodium (Catalog

No. C5793, Sigma-Aldrich, St. Louis, MO, USA) to establish a CAD animal model [14]. Two-dimensional ultrasound was employed using a small animal ultrasound system (Catalog No. Vevo 2100, FUJIFILM Visual Sonics Inc., Toronto, ON, Canada) to visualize the vascular orientation, lumen endoscopy, vessel wall thickness and plaque formation.

The thorax was directly sutured for the Sham group using surgical sutures (Catalog No. 11-0, Ethicon Inc., Somerville, NJ, USA), while animals subjected to modeling and atherosclerotic plaque formation were divided into the Model group and the Stent group (treatment with Meto-PLGA/PTMC DES), with 10 rabbits in each group. Pre-operatively, the Stent group received aspirin (Catalog No. A2093, Sigma-Aldrich, St. Louis, MO, USA) at 25 mg/day and clopidogrel (Catalog No. C3487, Sigma-Aldrich, St. Louis, MO, USA) at 12.5 mg/day. Three days post-operation, angiography was performed under X-ray fluoroscopy using the 1725AX small animal X-ray imaging system (Shanghai Yuyan Scientific Instrument Co. Ltd., Shanghai, China), with a microcatheter (Catalog No. MPC-1.2F, Cook Medical Inc., Bloomington, IN, USA) introduced and the DES positioned at the site of arterial stenosis. Routine intramuscular injections of 4.5 million U penicillin (Catalog No. P3032, Sigma-Aldrich, St. Louis, MO, USA) were administered for 3 days. After recovery, animals were housed in cages (Catalog No. RCC-01, Suzhou Fengshi Laboratory Animal Equipment Co., Ltd., Suzhou, China) and continued a high-fat diet (Catalog No. D12492, Research Diets Inc., New Brunswick, NJ, USA) for 30 days. The 1725AX small animal X-ray imaging system was sourced from Shanghai Yuyan Scientific Instrument Co. Ltd., China.

## 2.6 Serological Indicator Detection

Post-treatment, 3 mL of venous blood was collected from the ear margin using a 5 mL disposable syringe (Catalog No. 100500, Shanghai Kohama Medical Devices Co., Ltd., Shanghai, China) with a 22G needle (Catalog No. 302220, BD Medical, Franklin Lakes, NJ, USA), anticoagulated with heparin sodium (Catalog No. H3149, Sigma-Aldrich, St. Louis, MO, USA) at a final concentration of 10 U/mL and centrifuged at 1200 rpm for 10 min using a centrifuge (Catalog No. 5810R, Eppendorf AG, Hamburg, Germany). The supernatant was utilized to measure serum Interleukin-8 (IL-8) levels via radioimmunoassay using an IL-8 radioimmunoassay kit (Catalog No. RK00012, Shanghai Enzyme Linked Bio, Shanghai, China), while serum Vascular Cell Adhesion Molecule-1 (VCAM-1), Intercellular Adhesion Molecule-1 (ICAM-1) and Tumor Necrosis Factor-Alpha (TNF- $\alpha$ ) were assessed using a double-antibody sandwich ELISA methodology with VCAM-1 ELISA kit (Catalog No. EK0577, Shanghai Enzyme Linked Bio, Shanghai, China), ICAM-1 ELISA kit (Catalog No. EK0395, Shanghai Enzyme

Linked Bio, Shanghai, China) and TNF- $\alpha$  ELISA kit (Catalog No. EK0525, Shanghai Enzyme Linked Bio, Shanghai, China), respectively. The corresponding ELISA kits were sourced from Shanghai Enzyme Linked Bio, China.

## 2.7 Cardiac Function Testing

Twelve hours after treatment, the animals were anesthetized with 0.05 g/kg of 3% sodium pentobarbital (Sigma-Aldrich, USA). The right common carotid artery and left femoral artery were isolated. A polyethylene (PE-20) catheter was inserted through a right common carotid artery into the left ventricle, with the other end connected to a physiological recorder (Shanghai Renyi Biotechnology Co. China). This setup measured Left Ventricular Systolic Pressure (LVSP), LV end-diastolic pressure (LVEDP) and the maximum rates of pressure increase and decrease ( $\pm dp/dt_{max}$ ). Arterial systolic blood pressure (BPs) and diastolic BP (BPD) were assessed via catheterization of the left femoral artery.

## 2.8 Morphological Examination of Coronary Artery Tissue

Twenty-four hours after cardiac function assessment, the animals were euthanized under 3% sodium pentobarbital (Catalog No. P3761, Sigma-Aldrich, St. Louis, MO, USA) anesthesia. Coronary artery tissues were fixed in 4% paraformaldehyde (Catalog No. P6148, Sigma-Aldrich, St. Louis, MO, USA) for 24 hrs. Tissues were rinsed twice with PBS (pH 7.2, Catalog No. P1020, Solarbio Science & Technology Co., Ltd., Beijing, China), dehydrated through a graded ethanol series (50%: Catalog No. E7023-500ML, Sigma-Aldrich, St. Louis, MO, USA; 70%: Catalog No. 10009218, Sinopharm Chemical Reagent Co., Ltd., Shanghai, China; 80%: Custom-prepared, Sinopharm Chemical Reagent Co., Ltd., Shanghai, China; 90%: Custom-prepared, Sinopharm Chemical Reagent Co., Ltd., Shanghai, China; 100%: Catalog No. 10009218, Sinopharm Chemical Reagent Co., Ltd., Shanghai, China) and cleared in xylene (Catalog No. X1500, Solarbio Science & Technology Co., Ltd., Beijing, China). They were embedded in paraffin (Catalog No. P1461, Solarbio Science & Technology Co., Ltd., Beijing, China) using a tissue embedding machine (Catalog No. EG1150H, Leica Biosystems, Wetzlar, Germany) and sectioned into 4  $\mu$ m thick slices with a microtome (Catalog No. RM2235, Leica Biosystems, Wetzlar, Germany).

Staining was conducted according to the instructions of the Hematoxylin-Eosin staining kit (Catalog No. G1120, Shanghai Enzyme Linked Bio, Shanghai, China). The coronary artery tissue morphology was visualized via a CX23 Microscope (Olympus, Japan) equipped with a digital camera (Catalog No. DP27, Olympus, Tokyo, Japan) and image analysis software (Image-Pro Plus 6.0, Media Cybernetics, Rockville, MD, USA) was employed to evaluate intimal thickness, lumen area and stenosis severity.



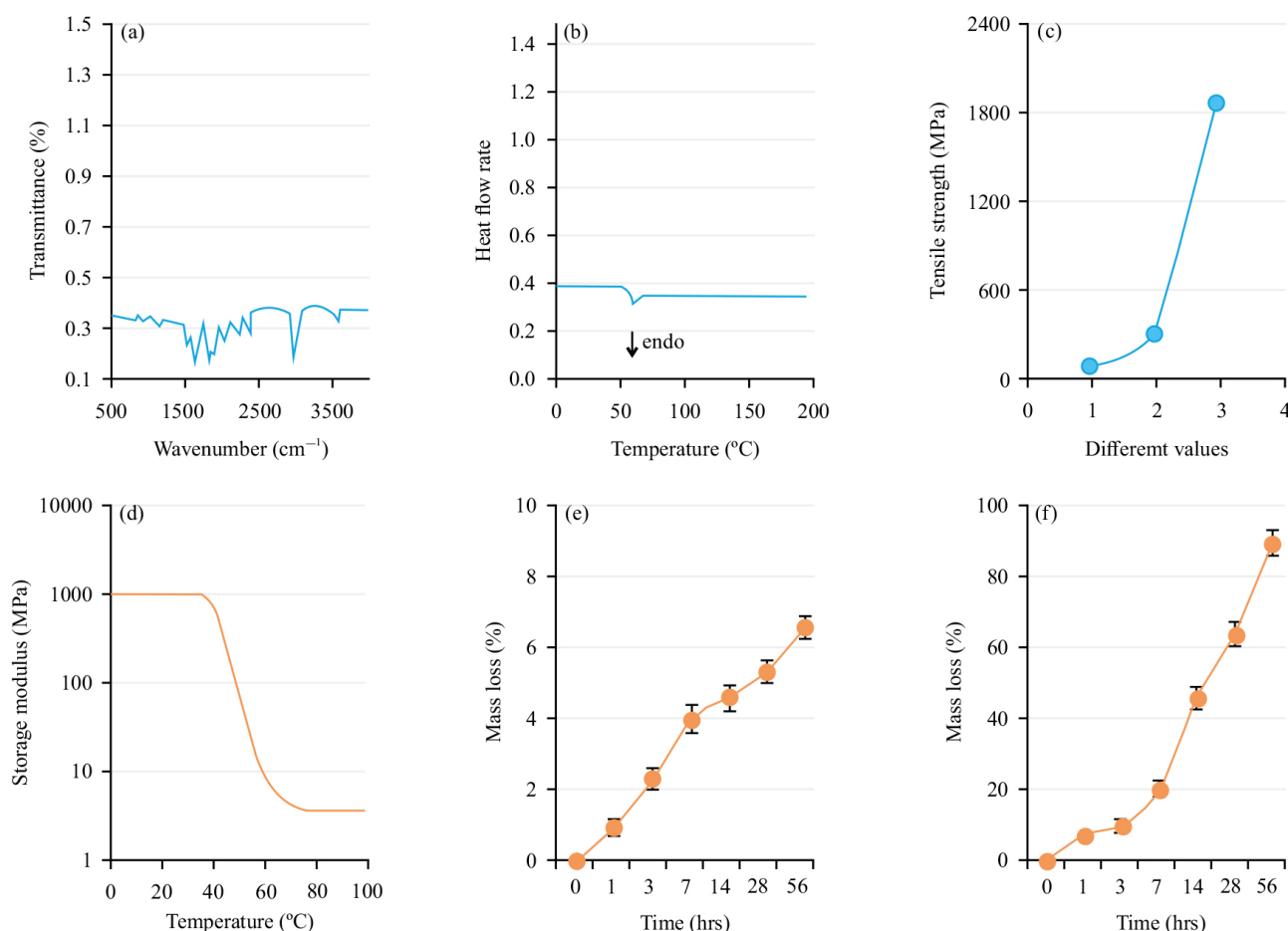


**Fig. 1. Physicochemical properties of Metoprolol-loaded poly (lactic-co-glycolic acid)-poly (trimethylene carbonate)-poly (glycolic acid) drug-eluting stent (Meto-PLGA/PTMC DES).** (a) Fourier Transform Infrared Spectroscopy (FTIR) spectrum; (b) Differential Scanning Calorimetry (DSC) curve; (c) Static mechanical properties (the x-axis labels 1, 2, and 3 represent the mass ratios of PLLA:PTMC:PGA as 1:1:1, 1:1:2 and 1:1:3, respectively); (d) Dynamic mechanical properties; (e) Weight loss versus time curve in water and (f) Weight loss versus time curve in proteinase K.

## 2.9 Statistical Methods

All data were presented as Mean  $\pm$  Standard Deviation and compared via One-way Analysis of Variance with *post hoc* LSD-*t* tests, performed using SPSS 22.0 (International Business Machines Corporation, Armonk, NY, USA). A  $p < 0.05$  meant statistically significant.

## 3. Results

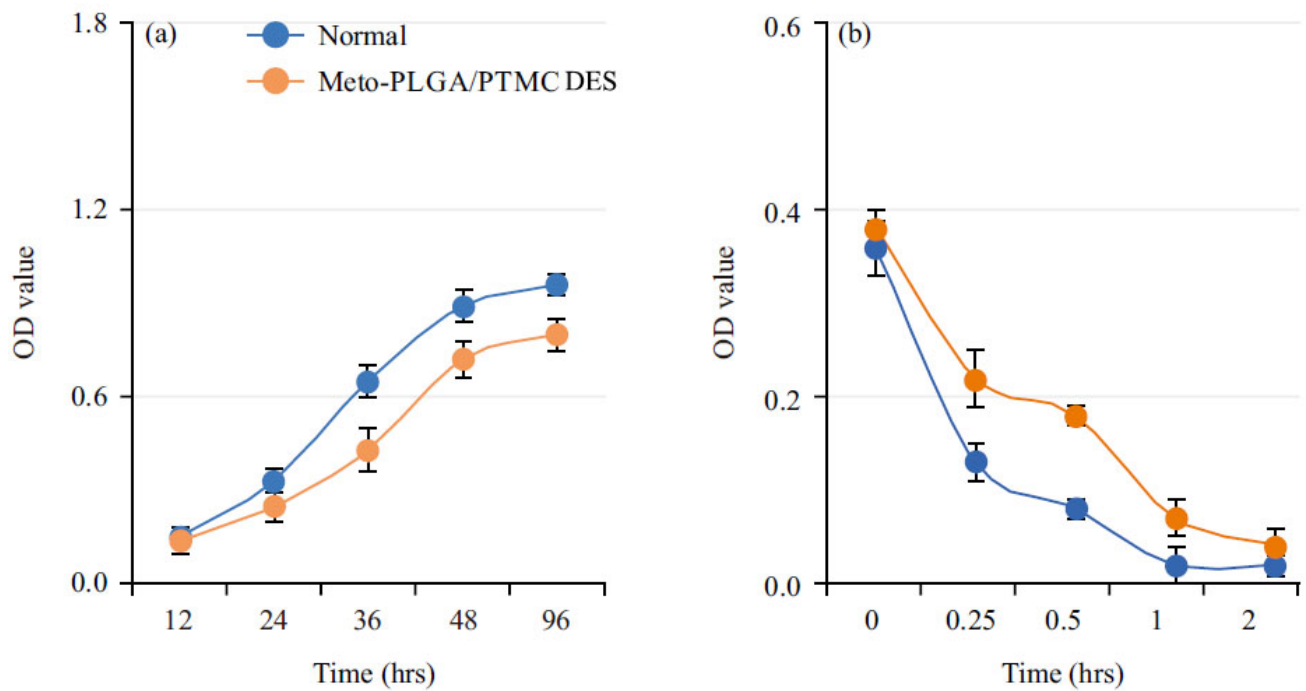
### 3.1 Physical and Chemical Performance Testing of Meto-PLGA/PTMC DES

Fig. 1a shows the Fourier Transform Infrared Spectroscopy (FTIR) spectrum of Meto-PLGA/PTMC DES. The spectrum indicated a notable presence of PLLA in Meto-PLGA/PTMC DES, with a prominent C = O peak at 1758/cm and a notable -CH<sub>2</sub> peak at 1431/cm. Fig. 1b depicts that the glass transition temperature (T<sub>g</sub>) of Meto-PLGA/PTMC DES is 56.9 °C. Fig. 1c presents the tensile strength is 1831.5 MPa. Fig. 1d illustrates the storage modulus of Meto-PLGA/PTMC DES as a function of tempera-

ture, showing a decreasing trend with increasing temperature, with a sharp decline in storage modulus observed above 40 °C. Fig. 1e displays the weight loss versus time curves for Meto-PLGA/PTMC DES during degradation in water and proteinase K. Over time, the weight loss of Meto-PLGA/PTMC DES increased gradually (Fig. 1e), with a higher weight loss rate in proteinase K compared to water (Fig. 1f).

### 3.2 Biocompatibility Testing of Meto-PLGA/PTMC DES

Fig. 2a shows the results of cell proliferation assays for rabbit cardiac fibroblasts cultured in a normal medium and in extracts from Meto-PLGA/PTMC DES. Over time, proliferation activity increased markedly in both conditions, with higher proliferation in the normal medium. The effect of Meto-PLGA/PTMC DES on cell proliferation was minimal, indicating good cytocompatibility and absence of cytotoxicity. The hemolysis rate of Meto-PLGA/PTMC DES was 3.09%, which was below the 5% threshold, in-



**Fig. 2.** Cell compatibility of Metoprolol-loaded poly (lactic-co-glycolic acid)-poly (trimethylene carbonate)-poly (glycolic acid) drug-eluting stent (Meto-PLGA/PTMC DES) complex. (a) Effect of Meto-PLGA/PTMC DES on the growth of rabbit cardiac fibroblasts and (b) Dynamic clotting time curve of Meto-PLGA/PTMC DES.

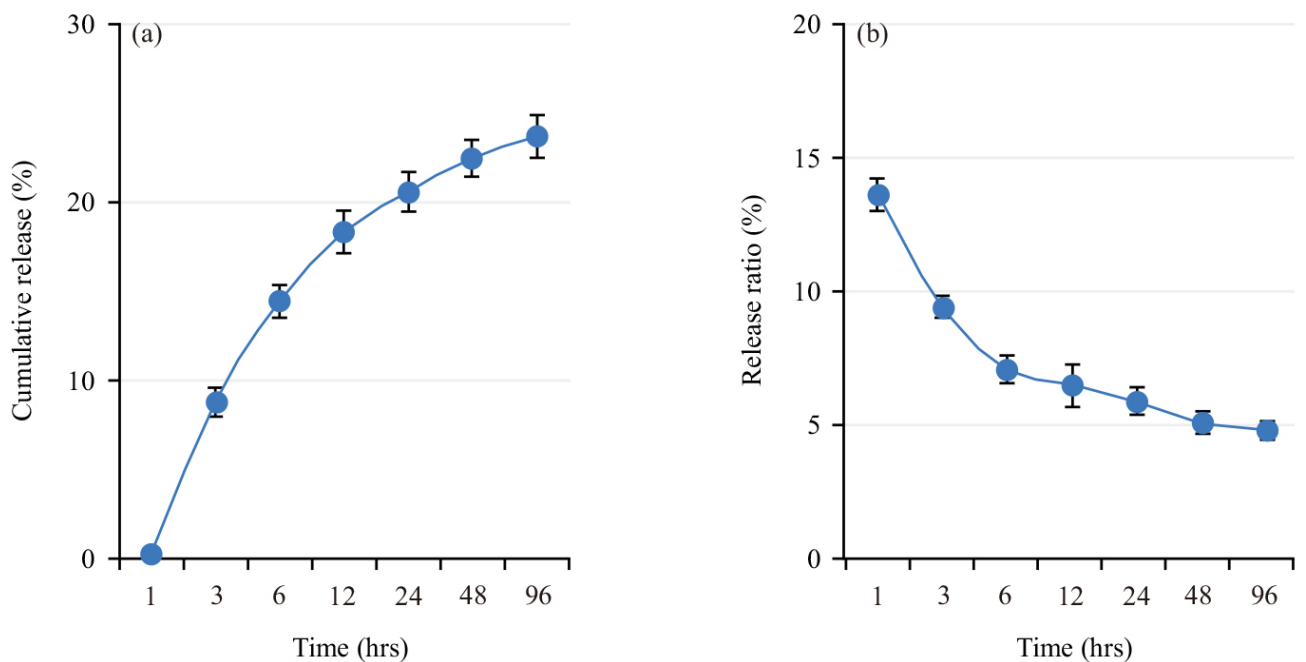


**Fig. 3.** *In vitro* drug release characteristics of Metoprolol-loaded poly (lactic-co-glycolic acid)-poly (trimethylene carbonate)-poly (glycolic acid) drug-eluting stent (Meto-PLGA/PTMC DES). (a) Cumulative drug release rate and (b) Amount of drug released.

dicating that the composite materials meet the hemolysis requirements for medical biomaterials. Fig. 2b presents the dynamic clotting time curve for Meto-PLGA/PTMC DES, which shows a similar gradual decrease as observed in the normal control, indicating comparable clotting behavior.

### 3.3 Meto-PLGA/PTMC DES *In Vitro* Drug Release Detection

Fig. 3 shows the *in vitro* drug release curve of Meto-PLGA/PTMC DES. Over time, the cumulative drug release rate of the stent gradually increased (Fig. 3a), while the to-

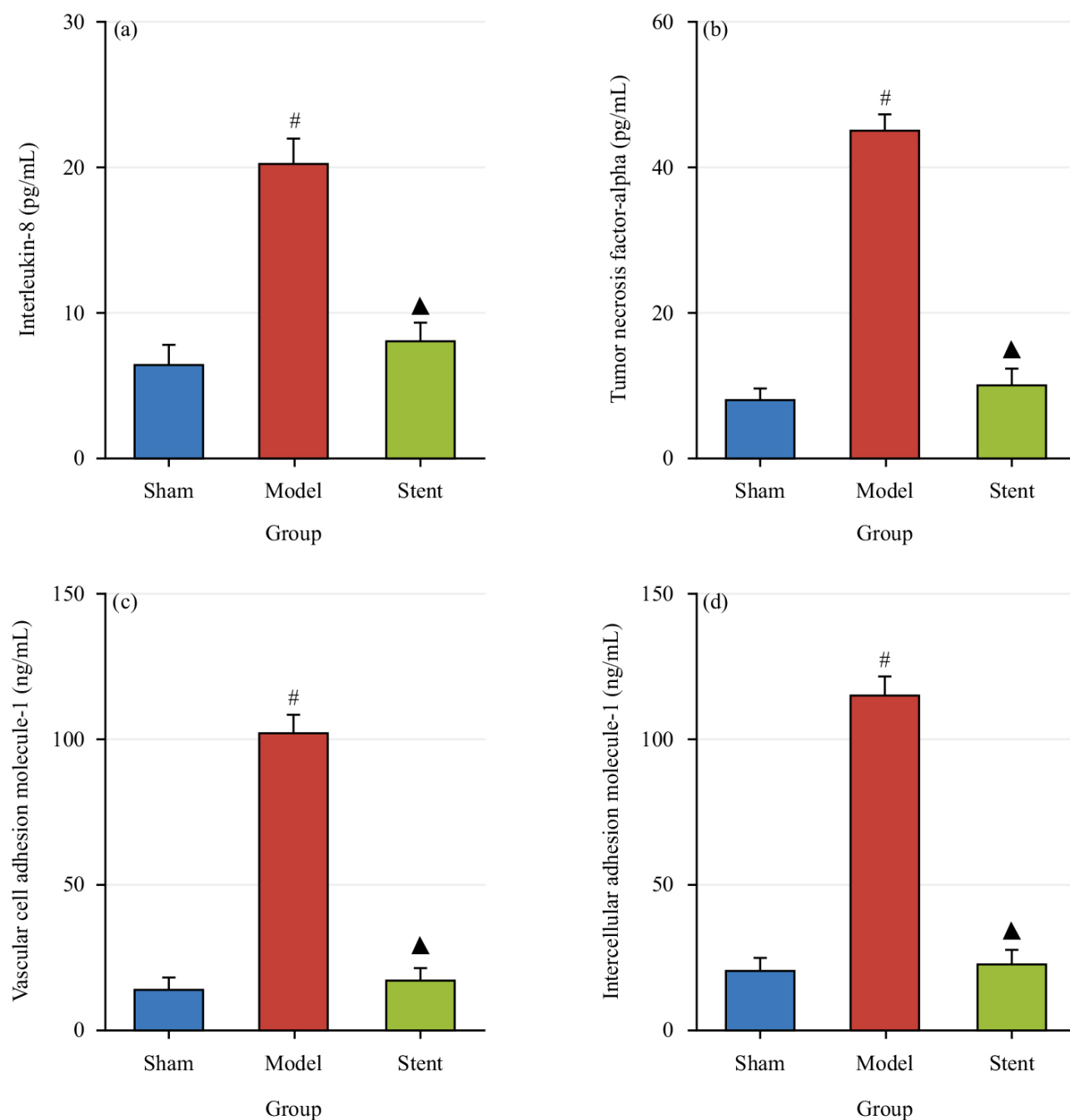


**Fig. 4. Contrast of serum levels of related factors across groups.** (a) Expression levels of Interleukin-8 (IL-8); (b) Expression levels of Tumor Necrosis Factor-Alpha (TNF- $\alpha$ ); (c) Expression levels of Vascular Cell Adhesion Molecule-1 (VCAM-1) and (d) Expression levels of Intercellular Adhesion Molecule-1 (ICAM-1). <sup>#</sup> $p < 0.05$  vs Sham group and <sup>▲</sup> $p < 0.05$  vs Model group.

tal amount of drug released gradually decreased (Fig. 3b), indicating that the stent enables slow and sustained drug release with a stable release profile.

### 3.4 Therapeutic Effect of Meto-PLGA/PTMC DES Implantation on Animals With Coronary Heart Disease

#### 3.4.1 Serum Inflammatory Marker Levels in Each Group

The changes in the expression levels of IL-8 (Fig. 4a), TNF- $\alpha$  (Fig. 4b), VCAM-1 (Fig. 4c) and ICAM-1 (Fig. 4d)

in the serum of animals from each group were measured. The results revealed that IL-8, TNF- $\alpha$ , VCAM-1 and ICAM-1 were greatly higher in Model group versus Sham group ( $p < 0.05$ ). These levels were substantially lower in Stent group versus Model group ( $p < 0.05$ ).

#### 3.4.2 Cardiac Function Parameters in Each Group

Fig. 5 shows the differences in cardiac function parameters LVSP (Fig. 5a), LVEDP (Fig. 5b),  $+dp/dt_{max}$

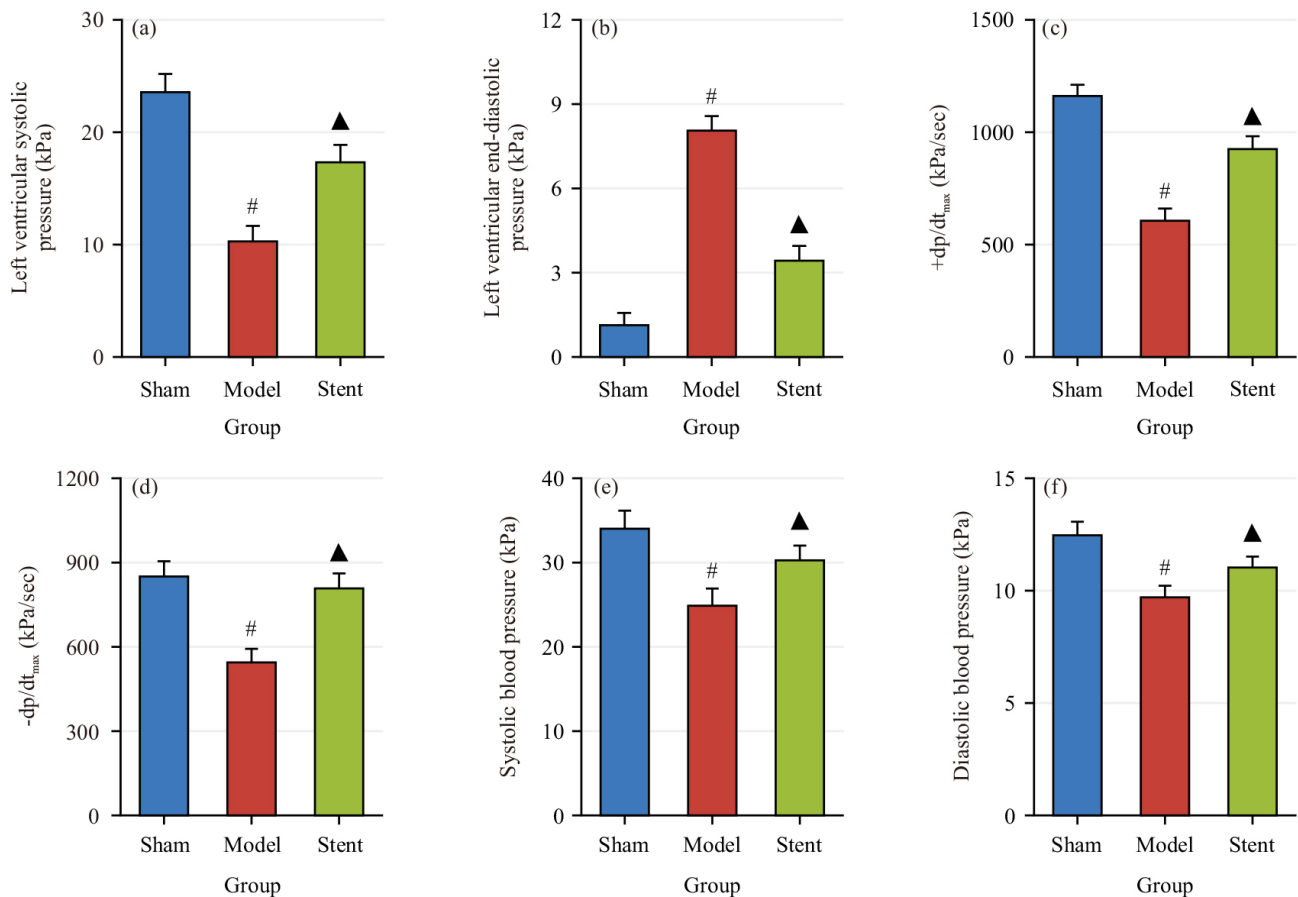


**Fig. 5. Comparison of cardiac function parameters across groups.** (a) Left Ventricular Systolic Pressure (LVSP); (b) LV end-diastolic pressure (LVEDP); (c) +dp/dt<sub>max</sub>; (d) -dp/dt<sub>max</sub>; (e) systolic blood pressure (BPs) and (f) diastolic BP (BPd). <sup>#</sup>*p* < 0.05 vs Sham group and <sup>▲</sup>*p* < 0.05 vs Model group.

(Fig. 5c), -dp/dt<sub>max</sub> (Fig. 5d), BPs (Fig. 5e) and BPd (Fig. 5f) across groups. In Model group, LVSP, +dp/dt<sub>max</sub>, -dp/dt<sub>max</sub>, BPs and BPd were drastically inferior to Sham group, while LVEDP was markedly higher (*p* < 0.05). In Stent group, LVSP, +dp/dt<sub>max</sub>, -dp/dt<sub>max</sub>, BPs and BPd were notably higher and LVEDP was greatly inferior to Model group (*p* < 0.05). The LVSP and LVEDP reflect cardiac contractility and diastolic dynamics, while ±dp/dt<sub>max</sub> measures ventricular pressure. These results indicated that Meto-PLGA/PTMC DES can greatly improve cardiac function in coronary heart disease animal models.

### 3.4.3 Coronary Artery Remodeling and Morphological Changes in Each Group

Fig. 6 shows the comparison of the intimal thickness (Fig. 6a), lumen area (Fig. 6b), intimal area (Fig. 6c) and degree of stenosis (Fig. 6d) across groups. The model group exhibited notably greater intimal thickness and area and considerably smaller lumen area relative to the Sham group (*p* < 0.05). The Stent group showed drastically reduced intimal thickness, area and stenosis degree, with a notably larger lumen area versus the Model group (*p* < 0.05).

## 4. Discussion

This work explores the potential adoption value of Meto-PLGA/PTMC DES in treating coronary heart disease. Experimental results demonstrated that Meto-PLGA/PTMC DES exhibited great advantages in terms of mechanical properties, biocompatibility, drug release characteristics, as well as anti-inflammatory and cardiovascular protective effects.

The PLLA-based material offers excellent biocompatibility and suitable mechanical properties, making it well-suited for cardiovascular stent development. Cardiovascular stents require materials with specific mechanical properties, such as stiffness, strength, elongation, recoil, compliance and degradability [15]. Previous studies confirmed that PLLA-based stent materials can withstand compression forces of 1.3 bars, similar to the strength of metal stents [16]. Kuriakose *et al.* [17] demonstrated that BPLPL-PLGA-based nanoparticles possess excellent physical and biological properties, making them viable as functional nanocarriers for the treatment and diagnosis of cardiovascular diseases. Kim *et al.* [18] reported that a polymer mixture of PLLA and phospholipid polymers is used for



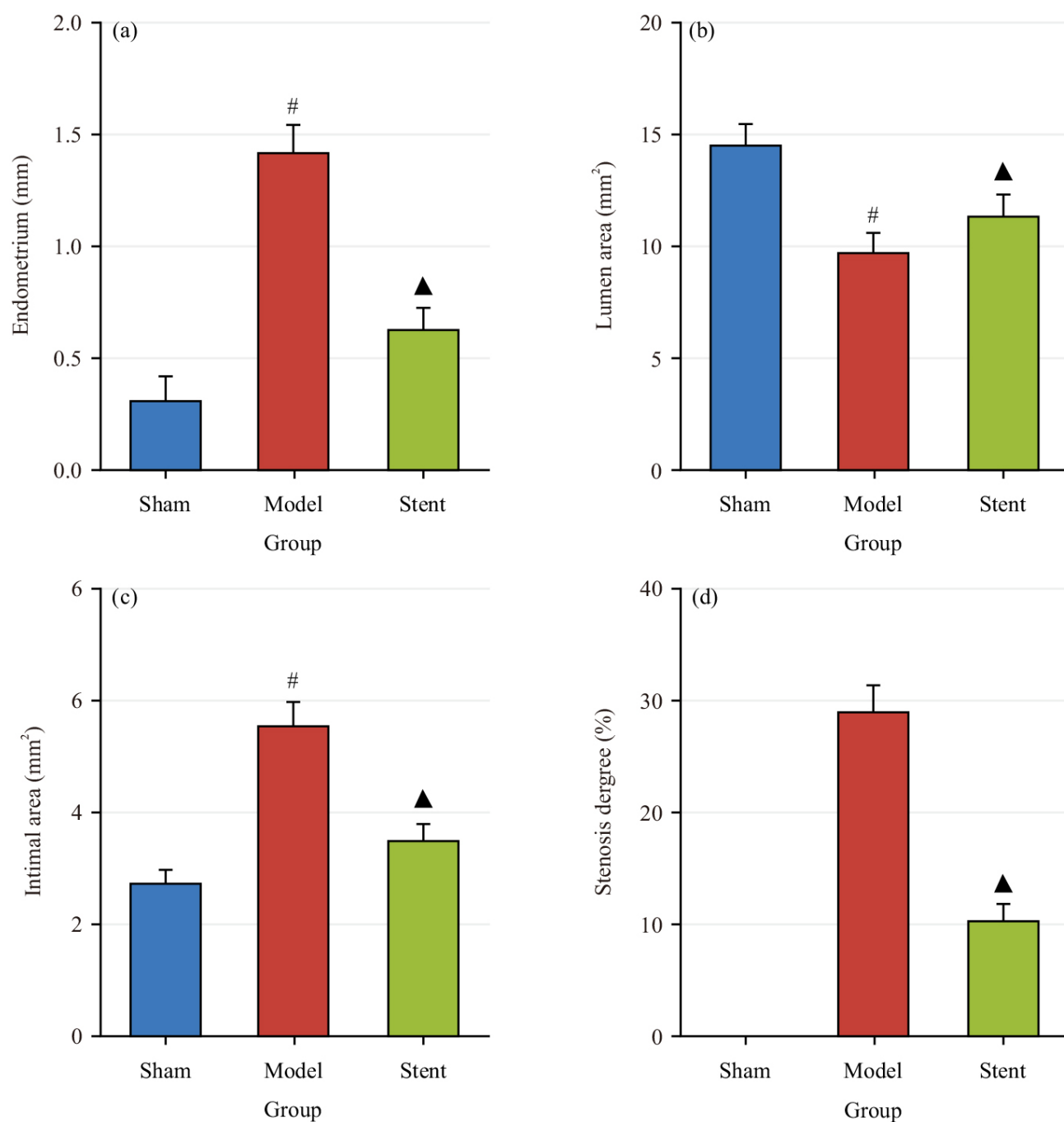


**Fig. 6. Comparison of coronary artery wall and intimal across groups.** (a) Intimal thickness; (b) Lumen area; (c) Intimal area and (d) Degree of stenosis. # $p < 0.05$  vs Sham group and ▲ $p < 0.05$  vs Model group.

biodegradable cardiovascular stents, while Kim *et al.* [19] also highlighted the use of PLLA material as a temporary scaffold for vascular walls. In this study, the glass Tg, tensile strength, elongation at break and Young's modulus of Meto-PLGA/PTMC DES demonstrated its sufficient mechanical strength and flexibility to withstand the complex stresses in the coronary blood flow dynamics. Particularly, the material's excellent cellular and blood compatibility suggested that the stent adapted well to the *in vivo* environment, reducing foreign body reactions and stent-related

complications. Young's modulus is a key physical property for evaluating a material's resistance to deformation [20]. The results indicated that Meto-PLGA/PTMC DES exhibited good tensile strength and deformation resistance. Viscoelasticity, a distinctive feature of polymer materials, shows strong time and temperature dependency [21]. The synthesized Meto-PLGA/PTMC DES had a Tg above 50 °C, maintaining a frozen molecular state within the normal body temperature range, thereby sustaining high mechanical strength. This study further confirmed the mechanical

performance and biocompatibility of Meto-PLGA/PTMC DES, highlighting its mechanical support advantages and its ability to maintain excellent cellular and blood compatibility even after drug loading. These findings align with existing literature and support the material's potential applications in the cardiovascular field.

Beta-blockers are highly effective in controlling ventricular arrhythmias associated with sympathetic nerve excitation, which can be triggered by acute myocardial ischemia, electrolyte disturbances and both psychological and physical stress, thus markedly preventing sudden cardiac death. In various acute coronary syndrome treatment guidelines, beta-blockers are prominently recommended both for acute management and long-term maintenance therapy, establishing them as one of the most used drugs in cardiovascular medicine [22,23]. Dransfield *et al.* [24] indicated that Meto is effective in preventing acute exacerbations of COPD. Dybro *et al.* [25] demonstrated that Meto reduces LV outflow tract obstruction at rest and during exertion and alleviates symptoms in patients. Heck *et al.* [26] reported that the beta-blocker Meto reduces myocardial troponin levels. Giannakopoulos and Noble [27] noted that early intravenous administration of beta-blockers is safe in hemodynamically stable patients and can prevent malignant arrhythmias. Meto can alleviate heart failure and atrial fibrillation [28,29]. As a widely applied beta-blocker, the sustained-release characteristics of Meto have been thoroughly validated in this study. Research on a CAD animal model demonstrated that Meto-PLGA/PTMC DES effectively inhibits the release of serum inflammatory factors. This not only confirms the anti-inflammatory effects of Meto but also highlights its potential in alleviating vascular inflammation and mitigating the progression of atherosclerosis in CAD. Mandal *et al.* [30] reported a myocardial infarction patient who, after receiving Meto and stent therapy, had stable vital signs. Beta-adrenergic blockers like Meto remain the preferred treatment for heart failure, CAD, atrial fibrillation and hypertension-related heart failure, angina or previous myocardial infarction [31]. Studies noted that patients undergoing percutaneous coronary interventions with balloon angioplasty and bare-metal stent implantation experience reduced IL-8 levels [32]. The stent materials used clinically must possess good biocompatibility characteristics, which primarily include cellular and hemocompatibility. Cellular biocompatibility involves evaluating the material's effects on cell adhesion, growth, differentiation and apoptosis. Blood compatibility requires assessing the material's anticoagulant properties to minimize thrombosis formation [33]. Thadani [34] demonstrated that stents coated with Meto have a positive impact on chronic stable angina. *In vitro* dynamic clotting time assays are used to assess the material's effect on coagulation function, primarily by measuring the activation of intrinsic coagulation factors. A dynamic clotting time curve that gradually declines over an extended period indicates superior anticoagulant perfor-

mance of the material. Stent implantation not only provides vascular support but also facilitates controlled drug release, enhancing the therapeutic effect of the stent by regulating the drug delivery [35]. The DES offer notable advantages, including significantly reduced restenosis rates, resistance to damage during expansion, independence from raw material supply and timing constraints and low implantation-related side effects [36].

The current study demonstrated that Meto-PLGA/PTMC DES markedly inhibited the release of serum inflammatory factors IL-8, TNF- $\alpha$ , VCAM-1 and ICAM-1 and enhanced cardiac function in animal models, achieving stable and prolonged therapeutic effects. This finding was in line with existing literature on the anti-inflammatory and cardiovascular protective effects of Meto. However, previous studies primarily focused on the effects of Meto administered orally or by injection. This study was the first to validate the sustained release properties and long-term therapeutic effects of Meto through a stent-loaded form, filling a gap in the research in this field. Additionally, this research extends the adoption of stent technology in the treatment of CAD, demonstrating the potential of drug release to improve coronary artery lesions. Traditional stents primarily focus on providing physical support. However, this study demonstrates that DES can simultaneously exert anti-inflammatory effects and prevent vascular remodeling, thereby offering a novel strategy for the comprehensive therapy of CAD. The findings of this study theoretically align well with the inflammation theory of atherosclerotic lesions. The anti-inflammatory action of Meto, achieved by reducing the expression of inflammatory factors, directly intervenes in coronary artery inflammation, which is consistent with the key mechanisms in the pathological process of atherosclerosis. Moreover, the sustained-release properties of the stent material further support the theory of maintaining effective drug concentrations locally over extended periods, contributing to the long-term prevention of restenosis.

## 5. Conclusion

The Meto-PLGA/PTMC DES demonstrated excellent cell and blood compatibility. When implanted at the site of CAD lesions in animal models, the sustained release of Meto effectively inhibited the release of serum inflammatory factors, suppressed neointimal hyperplasia and reduced the degree of vascular narrowing. This indicates that Meto plays a crucial anti-inflammatory and vascular protective role in the treatment of CAD. This work primarily focused on the short-term sustained-release effects of Meto and has not yet fully assessed the potential long-term impacts on CAD patients. Future research should address the long-term effects of Meto-eluting stents, including their impact on restenosis, thrombosis and patient quality of life.

## 6. Significance Statement

The Meto-PLGA/PTMC drug-eluting stent developed in this study offers an efficient and safe drug release solution, ensuring stable drug release while demonstrating exceptional mechanical strength and favorable blood compatibility. These characteristics are critical for enhancing the performance of medical implants. Furthermore, the drug-eluting stent has shown significant effects in reducing inflammation, improving cardiac function and alleviating coronary artery stenosis, presenting a promising new approach to the treatment of cardiovascular diseases. This research has the potential to advance the drug-eluting stent in coronary heart disease, thus providing safer and more effective therapeutic options for patients, with profound clinical and scientific significance.

## Availability of Data and Materials

All relevant data are within the paper and the relevant data be obtained from the first author or corresponding author upon reasonable request.

## Author Contributions

RL designed the research study. RL, AM and TA performed the research. RL, AM and TA provided help and advice on the ELISA experiments. RL, AM and TA analyzed the data. RL, AM and TA wrote, reviewed and revised the manuscript. All authors read and approved the final manuscript. All authors have participated sufficiently in the work and agreed to be accountable for all aspects of the work.

## Ethics Approval and Consent to Participate

The experimental protocol was approved by the Animal Ethical Committee of Kashi Prefecture Second People's Hospital (Xinjiang, China) (No. 2023-012). All the experimental protocols involved in the current investigation followed the Guide for the Care and Use of Laboratory Animals of the National Institutes of Health and the ARRIVE (Animal Research: Reporting of *in vivo* Experiments) guidelines.

## Acknowledgment

Not applicable.

## Funding

This work was supported by The Third Phase of The Tianshan Talent Program in Xinjiang Uygur Autonomous Region (No. 2021046).

## Conflict of Interest

The authors declare no conflict of interest.

## References

- [1] Katta N, Loethen T, Lavie CJ, Alpert MA. Obesity and Coronary Heart Disease: Epidemiology, Pathology, and Coronary Artery Imaging. *Current Problems in Cardiology*. 2021; 46: 100655. <https://doi.org/10.1016/j.cpcardiol.2020.100655>.
- [2] Muscella A, Stefano E, Marsigliante S. The effects of exercise training on lipid metabolism and coronary heart disease. *American Journal of Physiology. Heart and Circulatory Physiology*. 2020; 319: H76–H88. <https://doi.org/10.1152/ajpheart.00708.2019>.
- [3] Tsao CW, Vasan RS. Cohort Profile: The Framingham Heart Study (FHS): overview of milestones in cardiovascular epidemiology. *International Journal of Epidemiology*. 2015; 44: 1800–1813. <https://doi.org/10.1093/ije/dyv337>.
- [4] Tian Y, Deng P, Li B, Wang J, Li J, Huang Y, *et al.* Treatment models of cardiac rehabilitation in patients with coronary heart disease and related factors affecting patient compliance. *Reviews in Cardiovascular Medicine*. 2019; 20: 27–33. <https://doi.org/10.31083/j.rcm.2019.01.53>.
- [5] Shlofmitz E, Iantorno M, Waksman R. Restenosis of Drug-Eluting Stents: A New Classification System Based on Disease Mechanism to Guide Treatment and State-of-the-Art Review. *Circulation. Cardiovascular Interventions*. 2019; 12: e007023. <https://doi.org/10.1161/CIRCINTERVENTIONS.118.007023>.
- [6] Zhao J, Wang X, Wang H, Zhao Y, Fu X. Occurrence and predictive factors of restenosis in coronary heart disease patients underwent sirolimus-eluting stent implantation. *Irish Journal of Medical Science*. 2020; 189: 907–915. <https://doi.org/10.1007/s11845-020-02176-9>.
- [7] Hou Y, Li X, Wang X, Dong T, Yang J. The effect of Huoxue Huayu decoction on restenosis after percutaneous coronary intervention in patients with coronary heart disease: A protocol for systematic review and meta-analysis. *Medicine*. 2022; 101: e28677. <https://doi.org/10.1097/MD.00000000000028677>.
- [8] Kuramitsu S, Sonoda S, Ando K, Otake H, Natsuaki M, Anai R, *et al.* Drug-eluting stent thrombosis: current and future perspectives. *Cardiovascular Intervention and Therapeutics*. 2021; 36: 158–168. <https://doi.org/10.1007/s12928-021-00754-x>.
- [9] Chen YL, Fan J, Chen G, Cao L, Lu L, Xu Y, *et al.* Polymer-free drug-eluting stents versus permanent polymer drug-eluting stents: An updated meta-analysis. *Medicine*. 2019; 98: e15217. <https://doi.org/10.1097/MD.00000000000015217>.
- [10] Shore ND, Mehlhaff BA, Cookson MS, Saltzstein DR, Tutrone R, Brown B, *et al.* Impact of Concomitant Cardiovascular Therapies on Efficacy and Safety of Relugolix vs Leuprolide: Subgroup Analysis from HERO Study in Advanced Prostate Cancer. *Advances in Therapy*. 2023; 40: 4919–4927. <https://doi.org/10.1007/s12325-023-02634-7>.
- [11] Huang KY, Tseng PT, Wu YC, Tu YK, Stubbs B, Su KP, *et al.* Do beta-adrenergic blocking agents increase asthma exacerbation? A network meta-analysis of randomized controlled trials. *Scientific Reports*. 2021; 11: 452. <https://doi.org/10.1038/s41598-020-79837-3>.
- [12] Clezar CN, Flumignan CD, Cassola N, Nakano LC, Trevisani VF, Flumignan RL. Pharmacological interventions for asymptomatic carotid stenosis. *The Cochrane Database of Systematic Reviews*. 2023; 8: CD013573. <https://doi.org/10.1002/14651858.CD013573.pub2>.
- [13] Liu Y, Li Z, Dou L, Zhang Y, He S, Zhu J, *et al.* Autologous esophageal mucosa with polyglycolic acid transplantation and temporary stent implantation can prevent stenosis after circumferential endoscopic submucosal dissection. *Annals of Translational Medicine*. 2021; 9: 546. <https://doi.org/10.21037/atm-20-6987>.
- [14] Shiomi M. The History of the WHHL Rabbit, an Animal Model

of Familial Hypercholesterolemia (I) - Contribution to the Elucidation of the Pathophysiology of Human Hypercholesterolemia and Coronary Heart Disease. *Journal of Atherosclerosis and Thrombosis*. 2020; 27: 105–118. <https://doi.org/10.5551/jat.RV17038-1>.

- [15] Ostasevicius V, Tretsakou-Savich Y, Venslauskas M, Bertasiene A, Minchenya V, Chernoglaiz P. Adaptation of cardiovascular system stent implants. *Biomedizinische Technik. Biomedical Engineering*. 2018; 63: 279–290. <https://doi.org/10.1515/bmt-2017-0018>.
- [16] Hou Z, Yan W, Li T, Wu W, Cui Y, Zhang X, *et al.* Lactic acid-mediated endothelial to mesenchymal transition through TGF- $\beta$ 1 contributes to in-stent stenosis in poly-L-lactic acid stent. *International Journal of Biological Macromolecules*. 2020; 155: 1589–1598. <https://doi.org/10.1016/j.ijbiomac.2019.11.136>.
- [17] Kuriakose AE, Pandey N, Shan D, Banerjee S, Yang J, Nguyen KT. Characterization of Photoluminescent Polylactone-Based Nanoparticles for Their Applications in Cardiovascular Diseases. *Frontiers in Bioengineering and Biotechnology*. 2019; 7: 353. <https://doi.org/10.3389/fbioe.2019.00353>.
- [18] Kim HI, Ishihara K, Lee S, Seo JH, Kim HY, Suh D, *et al.* Tissue response to poly(L-lactic acid)-based blend with phospholipid polymer for biodegradable cardiovascular stents. *Biomaterials*. 2011; 32: 2241–2247. <https://doi.org/10.1016/j.biomaterials.2010.11.067>.
- [19] Kim HI, Takai M, Ishihara K. Bioabsorbable material-containing phosphorylcholine group-rich surfaces for temporary scaffolding of the vessel wall. *Tissue Engineering. Part C, Methods*. 2009; 15: 125–133. <https://doi.org/10.1089/ten.tec.2008.0307>.
- [20] Baba K, Mori Y, Chiba D, Kuwahara Y, Kurishima H, Tanaka H, *et al.* TiNbSn stems with gradient changes of Young's modulus and stiffness reduce stress shielding compared to the standard fit-and-fill stems. *European Journal of Medical Research*. 2023; 28: 214. <https://doi.org/10.1186/s40001-023-01199-z>.
- [21] Bellet P, Gasparotto M, Pressi S, Fortunato A, Scapin G, Mba M, *et al.* Graphene-Based Scaffolds for Regenerative Medicine. *Nanomaterials (Basel, Switzerland)*. 2021; 11: 404. <https://doi.org/10.3390/nano11020404>.
- [22] Dybro AM, Rasmussen TB, Nielsen RR, Ladefoged BT, Andersen MJ, Jensen MK, *et al.* Effects of Metoprolol on Exercise Hemodynamics in Patients With Obstructive Hypertrophic Cardiomyopathy. *Journal of the American College of Cardiology*. 2022; 79: 1565–1575. <https://doi.org/10.1016/j.jacc.2022.02.024>.
- [23] Paolillo S, Dell'Aversana S, Esposito I, Poccia A, Perrone Filardi P. The use of  $\beta$ -blockers in patients with heart failure and comorbidities: Doubts, certainties and unsolved issues. *European Journal of Internal Medicine*. 2021; 88: 9–14. <https://doi.org/10.1016/j.ejim.2021.03.035>.
- [24] Dransfield MT, Voelker H, Bhatt SP, Brenner K, Casaburi R, Come CE, *et al.* Metoprolol for the Prevention of Acute Exacerbations of COPD. *The New England Journal of Medicine*. 2019; 381: 2304–2314. <https://doi.org/10.1056/NEJMoa1908142>.
- [25] Dybro AM, Rasmussen TB, Nielsen RR, Andersen MJ, Jensen MK, Poulsen SH. Randomized Trial of Metoprolol in Patients With Obstructive Hypertrophic Cardiomyopathy. *Journal of the American College of Cardiology*. 2021; 78: 2505–2517. <https://doi.org/10.1016/j.jacc.2021.07.065>.
- [26] Heck SL, Mecinaj A, Ree AH, Hoffmann P, Schulz-Menger J, Fagerland MW, *et al.* Prevention of Cardiac Dysfunction During Adjuvant Breast Cancer Therapy (PRADA): Extended Follow-Up of a 2×2 Factorial, Randomized, Placebo-Controlled, Double-Blind Clinical Trial of Candesartan and Metoprolol. *Circulation*. 2021; 143: 2431–2440. <https://doi.org/10.1161/CIRCULATIONAHA.121.054698>.
- [27] Giannakopoulos G, Noble S. Should We Be Using Upstream Beta-Blocker Therapy for Acute Myocardial Infarction? *Current Cardiology Reports*. 2021; 23: 66. <https://doi.org/10.1007/s11886-021-01494-3>.
- [28] Piccini JP, Dufton C, Carroll IA, Healey JS, Abraham WT, Khaykin Y, *et al.* Bucindolol Decreases Atrial Fibrillation Burden in Patients With Heart Failure and the *ADRB1* Arg389Arg Genotype. *Circulation. Arrhythmia and Electrophysiology*. 2021; 14: e009591. <https://doi.org/10.1161/CIRC EP.120.009591>.
- [29] Piccini JP, Connolly SJ, Abraham WT, Healey JS, Steinberg BA, Al-Khalidi HR, *et al.* A genotype-directed comparative effectiveness trial of Bucindolol and metoprolol succinate for prevention of symptomatic atrial fibrillation/atrial flutter in patients with heart failure: Rationale and design of the GENETIC-AF trial. *American Heart Journal*. 2018; 199: 51–58. <https://doi.org/10.1016/j.ahj.2017.12.001>.
- [30] Mandal S, Pradhan RR, Mols Kowalczewski B. Atypical Presentation of Myocardial Infarction in a Young Patient With Polycystic Ovarian Syndrome. *Cureus*. 2020; 12: e9494. <https://doi.org/10.7759/cureus.9494>.
- [31] Dézsi CA, Szentes V. The Real Role of  $\beta$ -Blockers in Daily Cardiovascular Therapy. *American Journal of Cardiovascular Drugs: Drugs, Devices, and other Interventions*. 2017; 17: 361–373. <https://doi.org/10.1007/s40256-017-0221-8>.
- [32] Cortese B, Di Palma G, Guimaraes MG, Piraino D, Orrego PS, Buccheri D, *et al.* Drug-Coated Balloon Versus Drug-Eluting Stent for Small Coronary Vessel Disease: PICCOLETO II Randomized Clinical Trial. *JACC. Cardiovascular Interventions*. 2020; 13: 2840–2849. <https://doi.org/10.1016/j.jcin.2020.08.035>.
- [33] Gouëffic Y, Torsello G, Zeller T, Esposito G, Vermassen F, Hausegger KA, *et al.* Efficacy of a Drug-Eluting Stent Versus Bare Metal Stents for Symptomatic Femoropopliteal Peripheral Artery Disease: Primary Results of the EMINENT Randomized Trial. *Circulation*. 2022; 146: 1564–1576. <https://doi.org/10.1161/CIRCULATIONAHA.122.059606>.
- [34] Thadani U. Current medical management of chronic stable angina. *Journal of Cardiovascular Pharmacology and Therapeutics*. 2004; 9 Suppl 1: S11–S11–29; quiz S98–9. <https://doi.org/10.1177/107424840400900103>.
- [35] Jia B, Zhang X, Ma N, Mo D, Gao F, Sun X, *et al.* Comparison of Drug-Eluting Stent With Bare-Metal Stent in Patients With Symptomatic High-grade Intracranial Atherosclerotic Stenosis: A Randomized Clinical Trial. *JAMA Neurology*. 2022; 79: 176–184. <https://doi.org/10.1001/jamaneurol.2021.4804>.
- [36] Gao P, Wang T, Wang D, Liebeskind DS, Shi H, Li T, *et al.* Effect of Stenting Plus Medical Therapy vs Medical Therapy Alone on Risk of Stroke and Death in Patients With Symptomatic Intracranial Stenosis: The CASSISS Randomized Clinical Trial. *JAMA*. 2022; 328: 534–542. <https://doi.org/10.1001/jama.2022.12000>.